

ERA-40 Project Report Series

17. The ERA-40 Archive

Per Kållberg, Adrian Simmons, Sakari Uppala
and Manuel Fuentes

Series: ECMWF ERA-40 Project Report Series

A full list of ECMWF Publications can be found on our web site under:

<http://www.ecmwf.int/publications/>

Contact: library@ecmwf.int

© Copyright 2004

European Centre for Medium Range Weather Forecasts
Shinfield Park, Reading, RG2 9AX, England

Literary and scientific copyrights belong to ECMWF and are reserved in all countries. This publication is not to be reprinted or translated in whole or in part without the written permission of the Director. Appropriate non-commercial use will normally be granted under the condition that reference is made to ECMWF.

The information within this publication is given in good faith and considered to be true, but ECMWF accepts no liability for error, omission and for loss or damage arising from its use.

The ERA-40 Archive

Per Kållberg, Adrian Simmons, Sakari Uppala
and Manuel Fuentes

September 2004



1 Introduction

The primary objectives of ERA-40 were:

- (i) to produce and promote the use of a comprehensive set of global analyses describing the state of the atmosphere and land and ocean-wave conditions from during the 45 years from September 1957 to August 2002;
- (ii) to foster European and international research by making the observations, the analyses and the study reports widely available.

An essential element of this was the production of an archive of data. This is necessary both to support the re-analysis itself and to support the subsequent use of the observations, the analyses and the diagnostic information produced by the analysis process. The archive is designed to:

- preserve all primary data;
- serve the needs of the production system for the re-analysis;
- serve the needs of users; those with direct access to the full archive, those supported by ECMWF data services (<http://www.ecmwf.int/products/data/archive/index.html>)
- and those accessing the reduced resolution data on the Data Server (http://data.ecmwf.int/data/d/era40_daily/).

ERA-40 generated supported data sets, archived in ECMWF's Meteorological Archive and Retrieval System (MARS). The supported data comprise:

- observations;
- analysis and forecast fields from the assimilating atmospheric model at full resolution;
- analysis and forecast fields from the atmospheric model evaluated at standard pressure levels;
- analysis and forecast fields from the atmospheric model evaluated on isentropic and PV = ± 2 surfaces;
- analysis and forecast fields from the coupled ocean-wave model on its regular 1.5°x1.5° latitude/longitude grid;
- monthly means, variances and covariances;
- feedback from the data assimilation for each observation supplied to it;
- selected diagnostic and derived data.

Additional data were generated as part of the evaluation phase of the project. Some of these data may be included later within the supported archive.

The atmospheric model used for ERA-40 is known as IFS CY23r4. A comprehensive documentation about the ECMWF forecasting system (the code of which has been developed jointly with Météo-France.) can be found on the ECMWF website at <http://www.ecmwf.int/research/ifsdocs/CY23r4/index.html>.

ERA-40 had the following resolution:

- 60 levels in the vertical;
- T159 spherical-harmonic representation for basic dynamical fields;
- a reduced Gaussian grid with approximately uniform 125km spacing for surface and other grid-point fields.

Details of the way basic fields were post-processed to produce the output fields are given in the documentation. Reference should be made in particular to Chapter 2: *FULL-POS post-processing and interpolation*, of Part VI: *Technical and computational procedures*. The atmospheric model was coupled to an ocean-wave model which resolved 25 wave frequencies and 12 wave directions at the nodes of its 1.5° grid.

All archived ERA-40 data are available directly through MARS to users from ECMWF and from ECMWF Member and Cooperating States with access to the ECMWF computer system. Arrangements exist at a national level within some Members States to supply data to users within that state who do not have direct access to MARS. The National Center for Atmospheric Research (NCAR), a partner in the ERA-40 project, has a copy of the ERA-40 archive from which to provide UCAR members and non-UCAR research and educational institutions in the USA with data for scientific, research and educational uses. ERA-40 products are available from ECMWF Data Services, subject to the rules of data distribution adopted by the Council of ECMWF. Provision of observational data is subject to any restrictions imposed by the original suppliers of the data. The analysis data on the $2.5^{\circ} \times 2.5^{\circ}$ grid are available from ECMWF's public Data Server (<http://data.ecmwf.int/data>). The website should be consulted for a specification of the fields available.

MARS (see: <http://www.ecmwf.int/publications/manuals>) and ECMWF Data Services (see: <http://www.ecmwf.int/products/data>) support the supply of data on a range of grids. Data are either interpolated from archived values on the model's Gaussian grid, or evaluated from the archived spherical-harmonic representation.

2 Archive of observations

2.1 Observations available for use in ERA-40

The observational data used in ERA-40 include both data from the operational ECMWF archives and data supplied to ECMWF by external institutions for use in re-analysis. Externally supplied data have been stored in the format as received, with only minor representation changes to eliminate machine-dependent features. The complexity of these ascii/binary formats vary, and especially for the satellite observations decoding often involved the solving of observation-specific problems. Later versions of some datasets were received, some in response to problems identified during ERA-40 production. Conventional *in-situ* data held by NCAR were first converted by NCEP to an internal NCEP BUFR structure, and then supplied to ECMWF. Data from all sources and structures have been converted at ECMWF to the FM94 BUFR representation and stored in the Centre's mass storage system, ecfs, with the name of the source. A comprehensive documentation of the decoding and quality control of the satellite data can be found in Hernandez, (2004), available at <http://www.ecmwf.int/research/era/Products/index.html> and from there to 'Report Series'

The data sources and types are specified in Table 1 for the full period 1957-2002. As is explained in the next section non-satellite source data were inserted into a database called PREODB for use in the production assimilation. Data marked as having public availability can be disseminated subject to the rules of data distribution adopted by the Council of ECMWF. Data marked as having restricted availability have been provided to ECMWF under restrictions as to their use or supply to third parties, and thus cannot be made widely available.

**Table 1: Observations available for ERA-40**

Data supplier	Data source/ type	Period	Availability
ECMWF	Operational GTS data Reception via GTS including surface, radio-sonde, pilot, dropsonde, profiler, aircraft and cloud motion wind data Special datasets FGGE Final Level 2b	1979-2002 1979	Public
NCAR, ECMWF, LMD, NASA, NOAA NCAR ECMWF Remote Sensing Systems ECMWF EUMETSAT	Level 1b data NOAA TOVS/ HIRS/ MSU/ SSU Level 1c radiances NOAA VTPR NOAA TOVS/ HIRS/ MSU/ SSU NOAA ATOVS DMSP SSM/I DMSP SSM/I Reprocessed Meteosat CSR	1979-2002 1972-1978 1979-2002 1998-2002 1987-1998 1997-2002 1982-1988	Public Public Public Restricted Public Public
ECMWF Japan Meteorological Agency EUMETSAT	Satellite cloud motion winds Geostationary satellites via GTS Separate supply of operational GMS data Reprocessed Meteosat	1979-2002 1980-1993 1982-1988	Public
ECMWF	ESA/ERS scatterometer and altimeter data	1991-2001	Restricted
NCAR	COADS - Comprehensive Ocean-Atmosphere Data Set Snow dataset from former USSR Automatic Antarctic stations from University of Wisconsin	1950-1997 1966-1990 1980-1998	Public
NCAR/ NCEP	Radiosonde and pilot China Raobs Countries US Control France Misc Russia TD52 TD53 TD54 ON20 US Navy GATE/ TWERLE USAF ON29 Surface TD13 TD14 USSR USAF ON124 Aircraft Australian US Navy ON20 Sadler Rean-1 Cloud Motion Winds ON20 Rean-1	1957-1962 1957-1967 1957-1979 1957-1978 1957-1979 1957-1978 1960-1978 1960-1971 1957-1969 1957-1974 1962-1972 1966-1973 1974-1976 1973-1979 1973-1978 1957-1973 1957-1978 1957-1978 1973-1979 1976-1978 1971-1979 1970-1979 1962-1972 1960-1973 1957-1961 1973-1978 1967-1972 1973-1978	Public

Table 1: Observations available for ERA-40

Data supplier	Data source/ type	Period	Availability
NCEP	Operational GTS data Reception via GTS including surface, radiosonde, dropsonde, pilot, aircraft and cloud motion wind data	1980-1994	Public
US Navy	Surface, Radiosonde, Pilot and Aircraft	1985-1996	Public
Japan Meteorological Agency	Operational GTS data Reception via GTS including radiosonde, pilot and aircraft data	1975-1978 1980-1997	Public
Atmospheric Environment Service, Canada	Canadian snow depths	1950-1999	Public
British Antarctic Survey	Antarctic Surface	1950-1999	Public
Australian Bureau of Meteorology	Surface pressure from Australian operational analyses Synthetic surface pressures (PAOBS)	1972-1978 1979-1994	Public
Australian Bureau of Meteorology National Climate Centre	Australian Antarctic surface and radiosonde data	1947-1999	Public
Woods Hole Institute for Oceanography	Subduction buoys	1991-1993	Public
Pacific Marine Environmental Laboratory	TAO-buoy array	1993-1995	Public
Center for Ocean Atmospheric Prediction Studies	TOGA COARE dropsondes, base dropsondes and radiosondes	1992-1993	Public
NASA	TOMS total ozone	1978-2001	Public
NASA, NOAA, ECMWF	SBUV ozone profile	1978-2001	Public

2.2 Archive of input observations to the analysis

As may be inferred from the above table, many observations appear in more than one of the data sources. After organizing the data into six-hourly slots the data were processed from all the different sources into a helper database called PREODB. At the same time basic date and time checks were carried out and a simulated analysis preprocessing step (MAKECMA) performed.

The merging of the multiple data sources, elimination of (most) duplicate observations and other “cleaning” of the data was carried out before the analysis step using in-house “ODB” database software. The archive of these merged observations was created cycle by cycle as the production streams proceeded.

These data can be retrieved using the following parameters:

```
class=e4, expver=01, type=ai, expect=any, date=yyyymmdd, time=hh, stream=da,
obstype="see Table 2; Analysis Input", target="bufrfile"
```

They can be separated by a filter described in

http://www.ecmwf.int/publications/manuals/mars/guide/Frequently_Asked_Questions.html.

The VTPR and Meteosat reprocessed data used in the re-analysis are stored in ecfs.



2.3 Archive of analysis feedback information in relation to the use of observations

The ERA-40 data assimilation system produced a range of BUFR-encoded feedback data relating to each observation presented to it. The BUFR feedback data contains, in addition to the original input BUFR data, all relevant observation-related information gathered during the data-assimilation cycle. Each of the items of information forms a separate section. Thus, there may be up to seven main feedback sections, of which some may have a few subsections. Each of these sections/subsections starts by first declaring what it is, by using BUFR (unexpanded) descriptors followed by the actual information.

The feedback data include in particular the departures of background and analysis values from the observation. They also include information relating to the use of the observation by the system, for example the flags set by possible blacklisting of the data, the flags set by climatological and background screening checks and information fed back by the variational quality control. The feedback data thus provide a wealth of information concerning the characteristics of the data assimilation and observing systems. Their technical specification is given in the documentation of the observation-processing component of the data assimilation system. The BUFR feedback data are stored in MARS. Data are organized into sets for each six-hour analysis period, with one set for all conventional observations, and one set for each type of satellite data.

These data can be retrieved using the following parameters:

```
class=e4, expver=01, type=af, expect=any, date=yyyymmdd, time=hh, stream=da,
obstype="see Table 2; Feedback ", target="feedbackfile"
```

They can be separated by a filter described in

http://www.ecmwf.int/publications/manuals/mars/guide/Frequently_Asked_Questions.html.

Table 2: - Grouping of observations and obstype identifiers for MARS retrieval of analysis input and feedback data

Grouping of observations	Analysis Input (AI)	Analysis Feedback (AF)
Non satellite observations: surface radiosonde dropsonde profiler pilot aircraft Satellite cloud motion winds	bufr	fbconv
Radiance data: VTPR1, VTPR2 HIRS, MSU, SSU AMSU-A, AMSU-B	atov	fbrad1c
SSM/I Radiances:	ssbt	fbssmi
SSM/I Retrievals: 1D-Var retrievals of TCWV 1D-Var retrievals of surface wind speed	(not available)	fbssmi
Scatterometer winds	scat	fbscat
Ozone data: TOMS SBUV	reo3	fbreo3

Feedback information is available only from the variational analysis of the atmospheric state. There is no feedback information related to the use observations in the T_{2m} , RH_{2m} , soil moisture, snow and ocean-wave height analysis.

Externally produced analyses of sea-surface temperature and sea-ice fraction were used in ERA-40. These have been preserved in their original form, as well as in the processed model forms specified below in Section 3.4.

3 Analysis and forecast fields

3.1 Generation of results

The ERA-40 data assimilation and forecast suite produced:

- four analyses per day, for 00, 06, 12, and 18 UTC;
- two forecasts per day to 6 hours ahead, from 06 and 18 UTC;
- two forecasts per day to 36 hours ahead, from 00 and 12 UTC;

In addition, forecasts have been subsequently run to ten days ahead from 00 and 12 UTC.

The analysis and short-range forecast data have been archived in full. Forecast data have been archived at 3- and 6-hour range from 00, 06, 12 and 18UTC and also at 9-, 12-, 15-, 18-, 21-, 24-, 30- and 36-hour range from 00 and 12UTC. Forecasts on the public Data Server are only at the 6-hour range.

Fields from the atmospheric model have been archived either at their full T159 spectral resolution or on the corresponding Gaussian grid of the model, depending on their basic representation in the model. Fields from the coupled ocean-wave model are saved on its regular 1.5° latitude/longitude grid.

The T159 model's reduced Gaussian grid is symmetric about the equator, with a north-south separation which is close to uniform in latitude, with a spacing of about 1.121° . There are 80 points aligned along the Greenwich Meridian from equator to pole. The number of points in the east-west varies with latitude, with uniform grid spacing along a particular line of latitude. The spacing is 1.125° in the tropics. The grid is specified (for the Northern Hemisphere) in Table 3, which gives for each row the latitude (accurate to two decimal points) and the number of points in the east-west.

The WMO representation form FM92 GRIB is used to represent all analysis and forecast fields. In general, ERA GRIB data are coded using ECMWF's local versions of GRIB code table 2 (version number 128 for atmosphere products, 140 for wave products), which gives parameter names and units. An additional local version, 162, of GRIB code table 2 is used for atmospheric parameters not included in the standard version 128. They include the "Additional vertical integrals for energy, mass, water and ozone budgets" in section 3.5, the "Additional fields accumulated from the physical parametrizations" in section 3.7 and the "Transient variances and covariances" in section 4.2. All local ECMWF versions of GRIB code table 2 are tabulated in <http://www.ecmwf.int/services/archive>.

Table 3: The Gaussian grid

Row no.	Lat.	Points	Row no.	Lat.	Points	Row no.	Lat.	Points	Row no.	Lat.	Points
1	89.14	18	2	88.03	25	3	86.91	36	4	85.79	40
5	84.67	45	6	83.55	54	7	82.43	60	8	81.31	64
9	80.19	72	10	79.06	72	11	77.94	80	12	76.82	90
13	75.70	96	14	74.58	100	15	73.46	108	16	72.34	120
17	71.21	120	18	70.09	128	19	68.97	135	20	67.85	144
21	66.73	144	22	65.61	150	23	64.49	160	24	63.36	160
25	62.24	180	26	61.12	180	27	60.00	180	28	58.88	192
29	57.76	192	30	56.64	200	31	55.51	200	32	54.39	216
33	53.27	216	34	52.15	216	35	51.03	225	36	49.91	225
37	48.78	240	38	47.66	240	39	46.54	240	40	45.42	256
41	44.30	256	42	43.18	256	43	42.06	256	44	40.93	288
45	39.81	288	46	38.69	288	47	37.57	288	48	36.45	288
49	35.33	288	50	34.21	288	51	33.08	288	52	31.96	288
53	30.84	300	54	29.72	300	55	28.60	300	56	27.48	300
57	26.36	320	58	25.23	320	59	24.11	320	60	22.99	320
61	21.87	320	62	20.75	320	63	19.63	320	64	18.50	320
65	17.38	320	66	16.26	320	67	15.14	320	68	14.02	320
69	12.90	320	70	11.78	320	71	10.65	320	72	9.53	320
73	8.41	320	74	7.29	320	75	6.17	320	76	5.05	320
77	3.93	320	78	2.80	320	79	1.68	320	80	0.56	320

3.2 Upper air parameters on model and pressure levels

Upper-air data are saved at each of the 60 “full” model levels and at 23 pressure levels, except where stated otherwise. Model “half-level” pressures $p_{k-1/2}$ are defined by

$$p_{k-1/2} = A_{k-1/2} + B_{k-1/2} p_s$$

where p_s is surface pressure and $k=1,2,3,\dots,61$. The pressures of the “full” model levels, p_k , are defined by

$$p_k = \frac{1}{2}(p_{k-1/2} + p_{k+1/2})$$

Precise values for the $A_{k-1/2}$ and $B_{k-1/2}$ should be read from Section 2, the Grid Description Section, of a GRIB file for model-level data. Values accurate to five significant figures are given in Table 4, together with half and full level pressures for a surface pressure of 1013.25hPa. The corresponding heights, z_k , of the full levels are also shown, assuming a uniform scale height of 7km for pressure. For this scale height the model

level spacing is precisely 1.5km in the middle stratosphere. The 23 pressure levels to which the model-level fields are interpolated are also specified in Table 4.

Table 4: Model and pressure levels

k	Model Levels					Pressure levels (hPa)
	$A_{k-1/2}$ (hPa)	$B_{k-1/2}$	$p_{k-1/2}$ (hPa)	p_k (hPa)	z_k (km)	
1	0.00	0.00000	0.00	0.10	64.56	
2	0.20	0.00000	0.20	0.29	57.06	
3	0.38	0.00000	0.38	0.51	53.16	
4	0.64	0.00000	0.64	0.80	50.04	
5	0.96	0.00000	0.96	1.15	47.46	1
6	1.34	0.00000	1.34	1.58	45.27	
7	1.81	0.00000	1.81	2.08	43.33	2
8	2.35	0.00000	2.35	2.67	41.58	3
9	2.98	0.00000	2.98	3.36	39.96	
10	3.74	0.00000	3.74	4.19	38.41	
11	4.65	0.00000	4.65	5.20	36.90	5
12	5.76	0.00000	5.76	6.44	35.40	7
13	7.13	0.00000	7.13	7.98	33.90	
14	8.84	0.00000	8.84	9.89	32.40	10
15	10.95	0.00000	10.95	12.26	30.90	
16	13.56	0.00000	13.56	15.19	29.40	
17	16.81	0.00000	16.81	18.81	27.90	20
18	20.82	0.00000	20.82	23.31	26.40	
19	25.80	0.00000	25.80	28.88	24.90	30
20	31.96	0.00000	31.96	35.78	23.40	
21	39.60	0.00000	39.60	44.33	21.90	
22	49.07	0.00000	49.07	54.62	20.44	50
23	60.18	0.00000	60.18	66.62	19.05	70
24	73.07	0.00000	73.07	80.40	17.74	
25	87.65	0.00008	87.73	95.98	16.50	100
26	103.76	0.00046	104.23	113.42	15.33	
27	120.77	0.00182	122.61	132.76	14.23	
28	137.75	0.00508	142.90	154.00	13.19	150
29	153.80	0.01114	165.09	177.12	12.21	
30	168.19	0.02068	189.15	202.09	11.29	200

**Table 4: Model and pressure levels**

Model Levels						Pressure levels (hPa)
k	$A_{k-1/2}$ (hP)	$B_{k-1/2}$	$p_{k-1/2}$ (hPa)	p_k (hPa)	z_k (km)	
31	180.45	0.03412	215.03	228.84	10.42	
32	190.28	0.05169	242.65	257.36	9.59	250
33	197.55	0.07353	272.06	287.64	8.81	300
34	202.22	0.09967	303.22	319.63	8.08	
35	204.30	0.13002	336.04	353.23	7.38	
36	203.84	0.16438	370.41	388.27	6.71	400
37	200.97	0.20248	406.13	424.57	6.09	
38	195.84	0.24393	443.01	461.90	5.50	
39	188.65	0.28832	480.79	500.00	4.94	500
40	179.61	0.33515	519.21	538.591	4.42	
41	168.99	0.38389	557.97	577.38	3.94	
42	157.06	0.43396	596.78	616.04	3.48	600
43	144.11	0.48477	635.31	654.27	3.06	
44	130.43	0.53571	673.24	691.75	2.67	700
45	116.33	0.58617	710.26	728.16	2.31	
46	102.10	0.63555	746.06	763.20	1.98	775
47	88.02	0.68327	780.35	796.59	1.68	
48	74.38	0.72879	812.83	828.05	1.41	
49	61.44	0.77160	843.26	857.34	1.17	850
50	49.42	0.81125	871.42	884.27	0.95	
51	38.51	0.84737	897.11	908.65	0.76	
52	28.88	0.87966	920.19	930.37	0.60	925
53	20.64	0.90788	940.55	949.35	0.46	
54	13.86	0.93194	958.15	965.57	0.34	
55	8.55	0.95182	972.99	979.06	0.24	
56	4.67	0.96765	985.14	989.95	0.16	
57	2.10	0.97966	994.75	998.39	0.10	1000
58	0.66	0.98827	1002.02	1004.64	0.06	
59	0.07	0.99402	1007.26	1009.06	0.03	
60	0.00	0.99763	1010.85	1012.05	0.01	
61	0.00	1.00000	1013.25			

Table 5 gives details of the “upper air” parameters. These include surface geopotential and the logarithm of surface pressure. Although not strictly upper air parameters, these are produced in spherical-harmonic form along with the model level data. Surface pressure is needed to compute the distribution of pressure on the model surfaces as indicated above. The table indicates which parameters are stored at model levels and which are stored at pressure levels. The two horizontal representations are indicated by **sh** (spherical harmonics) and **gg** (Gaussian grid). Except where indicated, parameters are available from both analyses and forecasts. **Code** refers to the parameter reference number in GRIB code table 2, version 128. Note that the horizontal wind-components **Codes** 131/132 are not archived per se, they are evaluated from the archived vorticity and divergence by the MARS software when requested.

Table 5: - Upper Air Parameters on model and pressure levels

Parameter	Model levels		Pressure levels		Code	Units
	sh	gg	gg	sh		
potential vorticity			X		60	$\text{m}^2 \text{s}^{-1} \text{K kg}^{-1}$
surface geopotential ¹	X				129	$\text{m}^2 \text{s}^{-2}$
geopotential				X	129	$\text{m}^2 \text{s}^{-2}$
temperature	X			X	130	K
eastward wind component					131	m s^{-1}
northward wind component					132	m s^{-1}
specific humidity		X	X		133	kg/kg
vertical velocity	X			X	135	Pa s^{-1}
vorticity	X			X	138	s^{-1}
log surface pressure (Pa)	X				152	
divergence	X			X	155	s^{-1}
relative humidity				X	157	%
ozone mass mixing ratio		X	X		203	kg/kg
cloud liquid water content ²		X			246	kg/kg
cloud ice water content ²		X			247	kg/kg
cloud cover ²		X			248	(0-1)

1. analysis only

2. forecast only



3.3 Upper air parameters on isentropic and $PV=\pm 2$ surfaces

Fields have also been interpolated to fifteen isentropic surfaces. The potential temperatures of these surfaces are specified in Table 6, which also shows corresponding pressures and heights for a 250K dry isothermal atmosphere.

Table 6: - Isentropic levels and corresponding pressures and heights

θ (K)	p (hPa)	z (km)
265	815	1.5
275	716	2.4
285	632	3.4
300	528	4.7
315	445	5.9
330	378	7.1
350	308	8.6
370	254	10.0
395	202	11.7
430	150	13.9
475	106	16.4
530	72	19.2
600	47	22.4
700	27	26.4
850	14	31.3

Table 7 shows the parameters and horizontal representations of the fields archived on the isentropic surfaces.

Table 7: - Products on isentropic surfaces

Parameter	gg	sh	Code	Units
Montgomery potential		X	53	$m^2 s^{-2}$
pressure		X	54	Pa
potential vorticity	X		60	$m^2 s^{-1} K kg^{-1}$
eastward wind component			131	$m s^{-1}$
northward wind component			132	$m s^{-1}$
specific humidity	X		133	kg/kg
vorticity		X	138	s^{-1}
divergence		X	155	s^{-1}
ozone mass mixing ratio	X		203	kg/kg

Montgomery potential is defined as $\phi + c_{pd}\theta(p/p_0)^{\kappa_d}$, where ϕ and p are respectively the geopotential and the pressure of the constant- θ surface, c_{pd} is the specific heat of dry air at constant pressure and $\kappa_d = R_d/c_{pd}$, where R_d is the gas constant of dry air. Note, however, that θ is defined by $\theta = T(p/p_0)^{-\kappa}$, with κ defined for a moist atmosphere: $\kappa = R/c_p$, where $R = R_d(1 + (R_v/R_d - 1)q)$ and $c_p = c_{pd}(1 + (c_{pv}/c_{pd} - 1)q)$, with q the specific humidity, and R_v and c_{pv} respectively the gas constant and specific heat at constant pressure of water vapour. The effect of moisture is included also in the calculation of ϕ , as described in the documentation of the model.

Fields are also produced on a “PV= ± 2 ” surface on which the potential vorticity takes the value 2PVU in the northern hemisphere and -2PVU in the southern hemisphere (1PVU= $10^{-6}\text{m}^2\text{s}^{-1}\text{Kkg}^{-1}$), provided such a surface can be found searching downwards from the model level close to 96hPa. Values at this model level are used where the search is unsuccessful.

Table 8 shows the parameters archived on the PV= ± 2 surface. All fields are saved on the model’s Gaussian grid.

Table 8: - Products on the PV= ± 2 surface

Parameter	Code	Units
potential temperature	3	K
pressure	54	Pa
geopotential	129	$\text{m}^2 \text{s}^{-2}$
eastward wind component	131	m s^{-1}
northward wind component	132	m s^{-1}
specific humidity	133	kg/kg
ozone mass mixing ratio	203	kg/kg

3.4 Surface and single-level parameters

A variety of surface and single-level parameters are saved on the model’s Gaussian grid. The list of these differs according to whether they are produced by the analysis (**An**), or the forecast (**Fc**), and is given in Table 9 below. Forecast fields marked as (*accum.*) represent accumulated values, i.e. values integrated in time from the start over the range of the forecast.

Table 9: - Surface and single level parameters

Parameter	An	Fc	Code	Units
low vegetation cover	X		27	(0-1)
high vegetation cover	X		28	(0-1)
low vegetation type (table index)	X		29	index
high vegetation type (table index)	X		30	index
sea ice fraction	X		31	(0-1)
sea surface temperature	X		34	K
snow albedo	X	X	32	(0-1)

Table 9: - Surface and single level parameters

Parameter	An	Fc	Code	Units
snow density	X	X	33	kg
sea ice temperature layer 1	X	X	35	K
sea ice temperature layer 2	X	X	36	K
sea ice temperature layer 3	X	X	37	K
sea ice temperature layer 4	X	X	38	K
soil moisture level 1 (volumetric)	X	X	39	m ³ /m ³
soil moisture level 2 (volumetric)	X	X	40	m ³ /m ³
soil moisture level 3 (volumetric)	X	X	41	m ³ /m ³
soil moisture level 4 (volumetric)	X	X	42	m ³ /m ³
snow evaporation (<i>accum.</i>)		X	44	m
snow melt (<i>accum.</i>)		X	45	m
wind gusts at 10 m		X	49	ms ⁻¹
large-scale precipitation fraction (<i>accum.</i>)		X	50	s
surface geopotential	X		129	m ² s ⁻²
total column water	X	X	136	kg m ⁻²
total column water vapour	X	X	137	kg m ⁻²
soil temperature level 1	X	X	139	K
snow depth	X	X	141	m of water equivalent
large-scale precipitation (<i>accum.</i>)		X	142	m of water
convective precipitation (<i>accum.</i>)		X	143	m of water
snowfall (<i>accum.</i>)		X	144	m of water equivalent
boundary layer dissipation (<i>accum.</i>)		X	145	W m ⁻² s
surface sensible heat flux (<i>accum.</i>)		X	146	W m ⁻² s
surface latent heat flux (<i>accum.</i>)		X	147	W m ⁻² s
Charnock parameter	X	X	148	
mean sea level pressure	X	X	151	Pa
boundary layer height	X		159	m
standard deviation of orography	X		160	m
anisotropy of orography	X		161	
angle of sub-grid scale orography	X		162	
slope of sub-grid scale orography	X		163	
total cloud cover	X	X	164	(0-1)
10 metre eastward wind component	X	X	165	m s ⁻¹
10 metre northward wind component	X	X	166	m s ⁻¹

Table 9: - Surface and single level parameters

Parameter	An	Fc	Code	Units
2 metre temperature	X	X	167	K
2 metre dewpoint	X	X	168	K
downward surface solar radiation (<i>accum.</i>)		X	169	W m ⁻² s
soil temperature level 2	X	X	170	K
land/sea mask	X		172	(0,1)
surface roughness	X		173	m
albedo (climate)	X		174	
downward surface thermal radiation (<i>accum.</i>)		X	175	W m ⁻² s
surface solar radiation (<i>accum.</i>)		X	176	W m ⁻² s
surface thermal radiation (<i>accum.</i>)		X	177	W m ⁻² s
top solar radiation (<i>accum.</i>)		X	178	W m ⁻² s
top thermal radiation (<i>accum.</i>)		X	179	W m ⁻² s
eastward component of turbulent stress (<i>accum.</i>)		X	180	N m ⁻² s
northward component of turbulent stress (<i>accum.</i>)		X	181	N m ⁻² s
evaporation (<i>accum.</i>)		X	182	m of water
soil temperature level 3	X	X	183	K
low cloud cover	X	X	186	(0-1)
medium cloud cover	X	X	187	(0-1)
high cloud cover	X	X	188	(0-1)
sunshine duration since last post-processing step		X	189	s
latitudinal component of gravity wave stress (<i>accum.</i>)		X	195	N m ⁻² s
meridional component of gravity wave stress (<i>accum.</i>)		X	196	N m ⁻² s
gravity wave dissipation (<i>accum.</i>)		X	197	W m ⁻² s
skin reservoir content	X	X	198	m of water
maximum 2m temperature since last post-processing step		X	201	K
minimum 2m temperature since last post-processing step		X	202	K
runoff (<i>accum.</i>)		X	205	m of water
total column ozone	X	X	206	kg m ⁻²
top solar radiation clear sky (<i>accum.</i>)		X	208	W m ⁻² s
top thermal radiation clear sky (<i>accum.</i>)		X	209	W m ⁻² s
surface solar radiation clear sky (<i>accum.</i>)		X	210	W m ⁻² s
surface thermal radiation clear sky (<i>accum.</i>)		X	211	W m ⁻² s
instantaneous eastward component of turbulent stress		X	229	N m ⁻²
instantaneous northward component of turbulent stress		X	230	N m ⁻²

Table 9: - Surface and single level parameters

Parameter	An	Fc	Code	Units
instantaneous surface heat flux		X	231	W m ⁻²
instantaneous moisture flux (evaporation)		X	232	kg m ⁻² s
log. surface roughness length (m) for heat	X		234	
skin temperature	X	X	235	K
soil temperature level 4	X	X	236	K
snow temperature	X	X	238	K
convective snowfall (<i>accum.</i>)		X	239	m of water equivalent
large-scale snowfall (<i>accum.</i>)		X	240	m of water equivalent
forecast albedo		X	243	
forecast surface roughness		X	244	m
forecast log. surface roughness length (m) for heat		X	245	

3.5 Additional vertical integrals for energy, mass, water and ozone budgets

The standard model post-processing produced the surface and single-level fields given in Table 9. A number of additional “single-level” fields of vertical integrals relating to the budgets of mass, water, ozone and energy have been derived from the instantaneous post-processed model-level data. They are listed in Table 10. Further details are given in Annex 1.

Table 10: - Vertical integrals for budgets

Parameter	Definition	Code ¹	Units
mass of atmosphere	$\frac{1}{g} \int_0^1 \frac{\partial p}{\partial \eta} d\eta$	53	kg m ⁻²
temperature	$\frac{1}{g} \int_0^1 T \frac{\partial p}{\partial \eta} d\eta$	54	K kg m ⁻²
total column water vapour	$\frac{1}{g} \int_0^1 q \frac{\partial p}{\partial \eta} d\eta$	55	kg m ⁻²
total column liquid cloud water	$\frac{1}{g} \int_0^1 (CLW) \frac{\partial p}{\partial \eta} d\eta$	56	kg m ⁻²
total column frozen cloud water	$\frac{1}{g} \int_0^1 (CIW) \frac{\partial p}{\partial \eta} d\eta$	57	kg m ⁻²
total column ozone	$\frac{1}{g} \int_0^1 O_3 \frac{\partial p}{\partial \eta} d\eta$	58	kg m ⁻²
kinetic energy, <i>KE</i>	$\frac{1}{g} \int_0^1 \frac{1}{2} (\mathbf{v} \cdot \mathbf{v}) \frac{\partial p}{\partial \eta} d\eta$	59	J m ⁻²

Table 10: - Vertical integrals for budgets

Parameter	Definition	Code ¹	Units
thermal energy	$\frac{1}{g} \int_0^1 c_p T \frac{\partial p}{\partial \eta} d\eta$	60	J m ⁻²
dry static energy	$\frac{1}{g} \int_0^1 (c_p T + \phi_s) \frac{\partial p}{\partial \eta} d\eta$	61	J m ⁻²
moist static energy	$\frac{1}{g} \int_0^1 (Lq + c_p T + \phi_s) \frac{\partial p}{\partial \eta} d\eta$	62	J m ⁻²
total energy, <i>TE</i>	$\frac{1}{g} \int_0^1 (KE + Lq + c_p T + \phi_s) \frac{\partial p}{\partial \eta} d\eta$	63	J m ⁻²
energy conversion	$\frac{1}{g} \int_0^1 \frac{RT\omega}{p} \frac{\partial p}{\partial \eta} d\eta$	64	W m ⁻²
eastward mass flux	$\frac{1}{g} \int_0^1 u \frac{\partial p}{\partial \eta} d\eta$	65	kg m ⁻¹ s ⁻¹
northward mass flux	$\frac{1}{g} \int_0^1 v \frac{\partial p}{\partial \eta} d\eta$	66	kg m ⁻¹ s ⁻¹
eastward kinetic energy flux	$\frac{1}{g} \int_0^1 u \frac{1}{2} (\tilde{v} \cdot \tilde{v}) \frac{\partial p}{\partial \eta} d\eta$	67	W m ⁻¹
northward kinetic energy flux	$\frac{1}{g} \int_0^1 v \frac{1}{2} (\tilde{v} \cdot \tilde{v}) \frac{\partial p}{\partial \eta} d\eta$	68	W m ⁻¹
eastward heat flux	$\frac{1}{g} \int_0^1 u c_p T \frac{\partial p}{\partial \eta} d\eta$	69	W m ⁻¹
northward heat flux	$\frac{1}{g} \int_0^1 v c_p T \frac{\partial p}{\partial \eta} d\eta$	70	W m ⁻¹
eastward water-vapour flux	$\frac{1}{g} \int_0^1 u q \frac{\partial p}{\partial \eta} d\eta$	71	kg m ⁻¹ s ⁻¹
northward water-vapour flux	$\frac{1}{g} \int_0^1 v q \frac{\partial p}{\partial \eta} d\eta$	72	kg m ⁻¹ s ⁻¹
eastward geopotential flux	$\frac{1}{g} \int_0^1 u \phi \frac{\partial p}{\partial \eta} d\eta$	73	W m ⁻¹
northward geopotential flux	$\frac{1}{g} \int_0^1 v \phi \frac{\partial p}{\partial \eta} d\eta$	74	W m ⁻¹
eastward total energy flux	$\frac{1}{g} \int_0^1 u (TE) \frac{\partial p}{\partial \eta} d\eta$	75	W m ⁻¹

Table 10: - Vertical integrals for budgets

Parameter	Definition	Code ¹	Units
northward total energy flux	$\frac{1}{g} \int_0^1 v(TE) \frac{\partial p}{\partial \eta} d\eta$	76	W m ⁻¹
eastward ozone flux	$\frac{1}{g} \int_0^1 u O_3 \frac{\partial p}{\partial \eta} d\eta$	77	kg m ⁻¹ s ⁻¹
northward ozone flux	$\frac{1}{g} \int_0^1 v O_3 \frac{\partial p}{\partial \eta} d\eta$	78	kg m ⁻¹ s ⁻¹
divergence of mass flux	$\nabla \cdot \frac{1}{g} \int_0^1 \vec{v} \frac{\partial p}{\partial \eta} d\eta$	81	kg m ⁻² s ⁻¹
divergence of kinetic energy flux	$\nabla \cdot \frac{1}{g} \int_0^1 \frac{1}{2} (\vec{v} \cdot \vec{v}) \frac{\partial p}{\partial \eta} d\eta$	82	W m ⁻²
divergence of thermal energy flux	$\nabla \cdot \frac{1}{g} \int_0^1 \vec{v} c_p T \frac{\partial p}{\partial \eta} d\eta$	83	W m ⁻²
divergence of moisture flux	$\nabla \cdot \frac{1}{g} \int_0^1 \vec{v} q \frac{\partial p}{\partial \eta} d\eta$	84	kg m ⁻² s ⁻¹
divergence of geopotential flux	$\nabla \cdot \frac{1}{g} \int_0^1 \vec{v} \phi \frac{\partial p}{\partial \eta} d\eta$	85	W m ⁻²
divergence of total energy flux	$\nabla \cdot \frac{1}{g} \int_0^1 \vec{v} (TE) \frac{\partial p}{\partial \eta} d\eta$	86	W m ⁻²
divergence ¹ of ozone flux	$\nabla \cdot \frac{1}{g} \int_0^1 \vec{v} O_3 \frac{\partial p}{\partial \eta} d\eta$	87	kg m ⁻² s ⁻¹

1. All these budget integrals are defined by ECMWF local version 162 of GRIB code table 2

3.6 Ocean-wave data

A set of ocean-wave products has been generated by the wave analysis and coupled wave-model forecasts. They are archived together with fields of gridded data from the altimeters on the ERS-1 and ERS-2 satellites. The fields archived are listed in Table 11. **Code** refers to the parameter reference number in GRIB table 2, ECMWF local version 140. Data are stored on the wave model's 1.5° latitude/longitude grid.

Table 11: Wave Data - Analysis, forecasts and gridded ERS altimeter fields

Parameter	Code	Units
mean wave period from 1st moment	220	s
mean wave period from 2nd moment	221	s
wave spectral directional width	222	-
mean wave period from 1st moment of wind waves	223	s
mean wave period from 2nd moment of wind waves	224	s
wave spectral directional width of wind waves	225	-
mean wave period from 1st moment of swell	226	s
mean wave period from 2nd moment of swell	227	s
wave spectral directional width of swell	228	-
significant wave height	229	m
mean wave direction	230	degrees
peak period of 1d spectra	231	s
mean wave period	232	s
coefficient of drag with waves	233	
significant height of wind waves	234	m
mean direction of wind waves	235	degrees
mean period of wind waves	236	s
significant height of primary swell	237	m
mean direction of primary swell	238	degrees
mean period of primary swell	239	s
mean square slope of waves	244	
10m wind speed modified by wave model	245	m s ⁻¹
gridded ERS altimeter wave height ¹	246	m
gridded corrected ERS altimeter wave height ¹	247	m
gridded ERS altimeter range relative correction ¹	248	-
components of the 2D wave spectra	250	m ² s radians ⁻¹

1. Available from late 1991 onwards



3.7 Additional fields accumulated from the physical parametrizations

The data described in the following subsections are accumulated over the first three- and six-hour intervals of the forecasts carried out four times per day.

3.7.1 Parameters to support chemical-transport modelling

Table 12 indicates the fields produced for use in chemical-transport modelling and other trajectory studies.

Table 12: - Parameters to support chemical transport modelling (accumulated)

Parameter	Surfaces	Code ¹	Units
updraught mass flux	model half levels	104	kg m ⁻²
downdraught mass flux	model half levels	105	kg m ⁻²
updraught detrainment rate	model full levels	106	s m ⁻¹
downdraught detrainment rate	model full levels	107	s m ⁻¹
total precipitation profile	model half levels	108	kg m ⁻²
turbulent diffusion coefficient for heat	model half levels	109	m ²

1. GRIB code table 2 version 162

3.7.2 Radiative tendencies

Tendencies from cloudy and clear-sky radiation have been accumulated from the start of the forecast. The parameters indicated in Table 13 are saved at full model levels.

Table 13: - Parameters to validate clear sky radiation (accumulated)

Parameter	Code ¹	Units
Short wave radiative tendency	100	K
Long wave radiative tendency	101	K
Clear sky short wave radiative tendency	102	K
Clear sky long wave radiative tendency	103	K

1. GRIB code table 2 version 162

3.7.3 Net tendencies from parametrized processes

Net tendencies from parametrized processes have been accumulated for full model levels, as listed in Table 14.

Table 14: - Net Tendencies (accumulated)

Parameter	Code ¹	Units
u tendency	112	m s ⁻¹
v tendency	113	m s ⁻¹
T tendency	110	K
q tendency	111	kg/kg

1. GRIB code table 2 version 162

4 Monthly-means, variances and covariances

Monthly means of the analysed and forecast fields listed in section 3 were computed for each synoptic hour (00, 06, 12, or 18 UTC) separately and archived during production of the re-analyses. In MARS they are identified by **stream=mnth**. Monthly diurnal means (the average of the synoptic means) were also produced, **stream=moda**.

The monthly mean product parameters at model and pressure levels are the same as those listed in table 3.3. The monthly mean product parameters and levels for the isentropic and $PV=\pm 2$ surfaces are those listed in tables 3.4 and 3.5. Table 3.7 above lists the synoptic surface and single level parameters. There are a few exceptions from this table for the monthly means. These exceptions only are listed below in Table 15 in a similar format.

4.1 Monthly means of analyses

The synoptic monthly mean analysis at 00UTC and the monthly diurnal mean analysis both include the 00UTC analysis from the 1st day of the month. Hence, in view of the 3D-Var 'FGAT' configuration used for ERA-40, observations from 2101UTC on the last day of the previous month up to 2100UTC on the last day of the present month are actually used in producing the analyses on which the means are based. The synoptic monthly mean analyses at 06UTC, 12UTC and 18UTC are based on observations taken strictly within the month.

4.2 Monthly means of short-range (+3 and +6 hours) forecasts

Monthly mean forecast fields have been produced at forecast ranges of 3 and 6 hours. The monthly mean synoptic and monthly diurnal means at 3-hour range were prepared only for surface fields (table 3.7), in conjunction with the ECMWF/ISLSCP-II dataset (Section 6). They contain 3-hour forecasts from 00, 06, 12 and/or 18UTC strictly within the month.

The monthly mean 6-hour forecasts are averaged over all forecasts valid within the calendar month, thus the 00UTC synoptic mean and the diurnal mean each contain a 6-hour forecast initiated at 18UTC on the last day of the previous month. The rationale for this choice is that the mean of the 6-hour forecasts coincides with the mean analysis; it is exactly the mean of the 6-hour background forecasts used in the 3D-Var data assimilation for the month in question.

It should be pointed out that both the monthly mean and monthly diurnal mean 3 and 6-hour forecast accumulations in table 3.7 are accumulated over their respective forecast ranges. Thus, to get the precipitation in mm/day, the archived 6-hour accumulations should be multiplied by 1000*4. And the monthly/diurnal ('moda') 3-hour accumulation is a rather meaningless product even if available.

Table 15: - Monthly mean surface and single level parameters. Exceptions from table 3.7

Parameter	An	Fc	Code	Units
magnitude of surface stress		X	048	$N\ m^{-2}\ s$
wind gusts at 10 m	no mean	no mean	049	
land/sea mask	X	X	172	(0,1)
max. temp. at 2 m since previous post-processing	no mean	no mean	201	
min. temp. at 2 m since previous post-processing	no mean	no mean	202	
10 metre wind speed	X	X	207	$m\ s^{-1}$



4.3 Diurnal forecast accumulations from short-range forecasts

A separate set of monthly diurnal (**stream=moda**) means of 29 accumulated fluxes at the surface and at the top of the atmosphere has also been produced from the 6, 12, 24 and 36 hour short-range forecasts.

These means have been summed in such a way that the fluxes are accumulated within the exact limits of the calendar month, for instance the accumulated rain falling from 00UTC on the first day of the month to 24UTC on the last day. They are thus summed from different initial states depending on the different forecast ranges.

The monthly diurnal flux means are available at the 6 hour range summed from the four 6 hour forecasts each day; at the 12 hour range summed from the twice daily 12 hour forecasts from 00UTC and 12UTC; at 24 hour range summed from the twice daily 12-hour accumulations from +12 to +24 hours into the forecasts, and at the 36 hour range similarly summed from the twice daily 12-hour accumulations from +24 to +36 hours into the forecasts.

The parameters and units in the monthly flux dataset are listed in Table 16. Since the hydrological parameters are in units of m of water per day, they should be multiplied by 1000 to convert to kg/(m²day) or mm/day. Turbulent energy, radiation and momentum flux accumulations should be divided by 24 hours (86400 seconds) to get the commonly used units W m⁻² and N m⁻²

Table 16: Monthly-daily mean fluxes from +06, +12, +24 and +36 hour forecasts

Parameter	Code	Units
snow evaporation	044	m of water / day
snowmelt	045	m of water / day
magnitude of surface stress. +06h only	048	N m ⁻² s
large-scale precipitation fraction	050	s
stratiform precipitation	142	m of water / day
convective precipitation	143	m of water / day
snowfall	144	m of water / day
boundary layer dissipation	145	W m ⁻² s
surface sensible heat flux	146	W m ⁻² s
surface latent heat flux	147	W m ⁻² s
downward surface solar radiation	169	W m ⁻² s
downward surface thermal radiation	175	W m ⁻² s
surface solar radiation	176	W m ⁻² s
surface thermal radiation	177	W m ⁻² s
top solar radiation	178	W m ⁻² s
top thermal radiation	179	W m ⁻² s
eastward turbulent stress	180	N m ⁻² s
northward turbulent stress	181	N m ⁻² s
evaporation	182	m of water / day

Table 16: Monthly-daily mean fluxes from +06, +12, +24 and +36 hour forecasts

Parameter	Code	Units
eastward gravity wave stress	195	N m ⁻² s
northward gravity wave stress	196	N m ⁻² s
gravity wave dissipation	197	W m ⁻² s
runoff	205	m of water / day
top net solar radiation, clear sky	208	W m ⁻² s
top net thermal radiation, clear sky	209	W m ⁻² s
surface net solar radiation, clear sky	210	W m ⁻² s
surface net thermal radiation, clear sky	211	W m ⁻² s
convective snowfall	239	m of water / day
large-scale snowfall	240	m of water / day

4.4 Transient variances and covariances

A set of transient variances and covariances have been produced, with respect to the means for each of the four synoptic hours (**stream=msdc**) and for the full day (**stream=msda**). Parameters are specified in Table 17. Here the overbar denotes the relevant monthly mean, and x' denotes the deviation of field x from \bar{x} . ϕ denotes geopotential, u the eastward velocity component, v the northward velocity component, ω the pressure-coordinate vertical velocity, T temperature, q specific humidity, r relative humidity and O_3 ozone..

Table 17: Variances and co-variances

Parameter	Model levels	Pressure levels	Code ¹	Units
$\overline{\phi'\phi'}$		X	206	m ⁴ s ⁻⁴
$\overline{\phi'T}$		X	207	m ² K s ⁻²
$\overline{T'T}$	X	X	208	K ²
$\overline{\phi'q'}$		X	209	m ² s ⁻²
$\overline{T'q'}$	X	X	210	K
$\overline{q'q'}$	X	X	211	
$\overline{u'\phi'}$		X	212	m ³ s ⁻³
$\overline{u'T}$	X	X	213	m s ⁻¹ K
$\overline{u'q'}$	X	X	214	m s ⁻¹
$\overline{u'u'}$	X	X	215	m ² s ⁻²
$\overline{v'\phi'}$		X	216	m ³ s ⁻³
$\overline{v'T}$	X	X	217	m s ⁻¹ K
$\overline{v'q'}$	X	X	218	m s ⁻¹
$\overline{u'v'}$	X	X	219	m ² s ⁻²

Table 17: Variances and co-variances

Parameter	Model levels	Pressure levels	Code ¹	Units
$\overline{v'v'}$	X	X	220	$\text{m}^2 \text{s}^{-2}$
$\overline{\omega'\phi'}$		X	221	$\text{m}^2 \text{Pa s}^{-3}$
$\overline{\omega'T'}$	X	X	222	$\text{Pa s}^{-1} \text{K}$
$\overline{\omega'q'}$	X	X	223	Pa s^{-1}
$\overline{\omega'u'}$	X	X	224	m Pa s^{-2}
$\overline{\omega'v'}$	X	X	225	m Pa s^{-2}
$\overline{\omega'\omega'}$	X	X	226	$\text{Pa}^2 \text{s}^{-2}$
$\overline{p_s'p_s'}$	X		227	Pa^2
$\overline{r'r'}$		X	229	
$\overline{u'O_3'}$	X	X	230	m s^{-1}
$\overline{v'O_3'}$	X	X	231	m s^{-1}
$\overline{\omega'O_3'}$	X	X	232	Pa s^{-1}
$\overline{O_3'O_3'}$	X	X	233	

1. GRIB code table 2 version 162

5 Zonal-mean and grid-point diagnostics

The assimilating model has the capability to produce diagnostic output for specified individual grid-points and for averages over specified areas and along complete lines of latitude. These “DDH” (Diagnostic sur Domaines Horizontaux) data include tendencies from individual components of the physical parametrizations.

Sets of DDH diagnostics have been archived for the short-range ERA-40 forecasts. Due to their model-specific nature and non-standard format it is not planned that they be “supported data” in the sense that they be made available as part of the general data service to the user community at large. Consideration will be given to supporting subsets of the data depending on basic validation results, user demand and the availability of resources.

The data are:

- a set of zonal-mean diagnostics;
- a set of 27 point and 31 area-mean diagnostics, defined especially to cover major field-experiment sites and river basins. An illustration of the locations of points and areas is presented in Figure 1 , and precise specifications are given in Table 18.

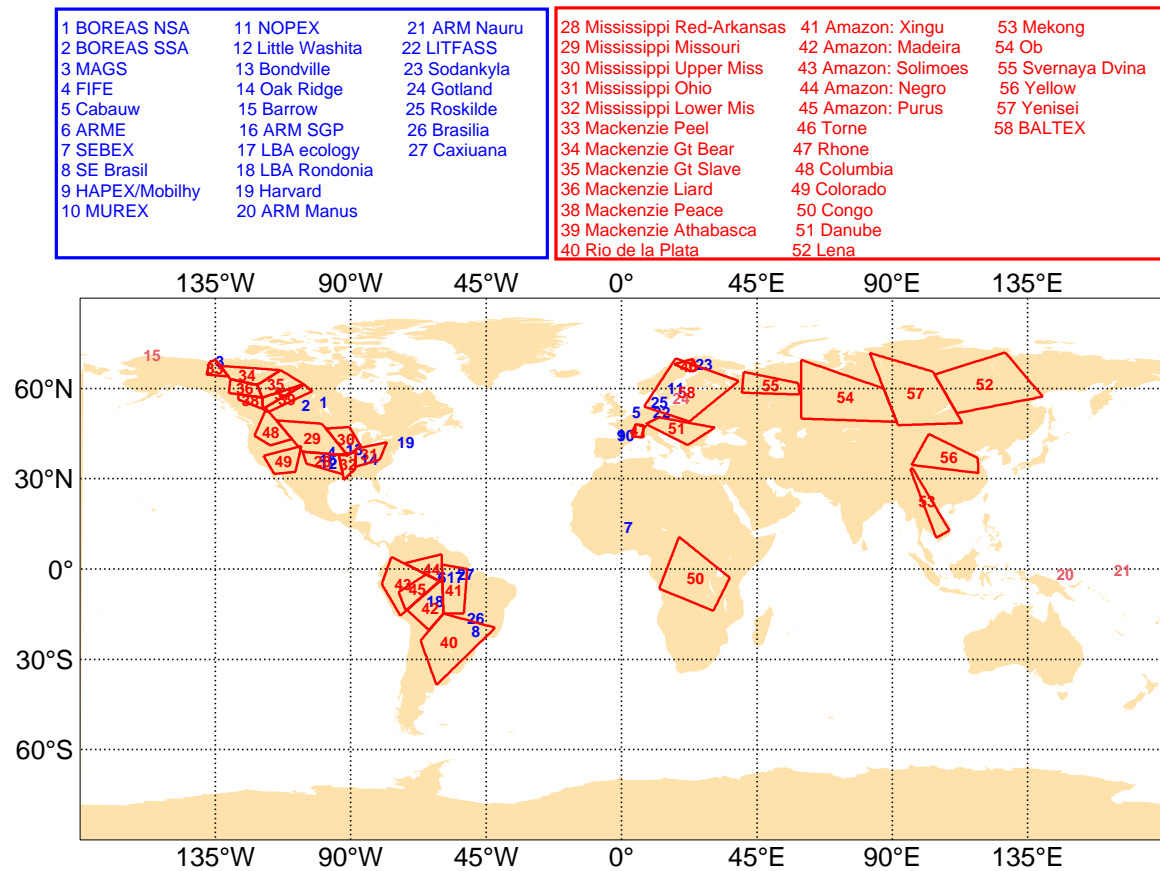


Figure 1 Points and areas for which detailed local (“DDH”) diagnostics are produced.

Table 18: Points and areas for the DDH diagnostics

	Description	Point (P) / Area (A)	Location (Lon,Lat)
1	BOREAS NSA	P	261.50, 55.90
2	BOREAS SSA-OBS	P	255.00, 54.00
3	MAGS: Tundra/forest	P	226.50, 68.75
4	FIFE	P	263.47, 39.05
5	Cabauw (Netherlands)	P	5.60, 51.94
6	ARME	P	300.05, -2.50
7	SEBEX	P	2.50, 13.50
8	South-east Brazil: Sugar Cane	P	311.93, -21.10
9	HAPEX/MOBILHY	P	359.90, 44.00
10	Toulouse (MUREX)	P	1.50, 44.20
11	NOPEX	P	17.29, 60.50
12	Little Washita (T. Meyers)	P	262.02, 34.96
13	Illinois (T.Meyers); also SURFRAD Bondville	P	271.71, 40.02
14	Oak Ridge (T.Meyers); also SURFRAD Bondville	P	275.71, 35.96
15	ARM Barrow (Alaska)	P	204.00, 71.00
16	ARM Southern Great Plains	P	262.70, 36.37
17	LBA: NASA ecology tower (undisturbed forest)	P	305.00, -2.86
18	LBA wet: Rondonia	P	298.10, -10.80
19	Harvard deciduous forest (S. Wofsky)	P	287.83, 42.53
20	ARM Tropics (Manus)	P	147.42, -2.06
21	ARM Tropics (Nauru Island)	P	166.92, -0.53
22	LITFASS (Germany)	P	14.06, 52.18
23	Sodankylä, Finland	P	26.65, 67.37
24	Östergarnsholm, Gotland (Baltic Sea)	P	19.50, 57.00
25	Risø (Roskilde)	P	12.10, 55.65
26	Brasilia: Cerrado	P	312.12, -15.95
27	Caxiuma: Forest site	P	308.55, -1.75
28	Mississippi: Red-Arkansas	A	254.00, 39.00 / 266.00, 37.90 267.40, 31.50 / 255.30, 35.00
29	Mississippi: Missouri	A	245.70, 49.40 / 260.40, 48.30 268.50, 37.80 / 254.00, 39.00
30	Mississippi: Upper Mississippi	A	262.00, 46.70 / 269.60, 47.20 273.30, 41.20 / 268.50, 37.80

Table 18: Points and areas for the DDH diagnostics

	Description	Point (P) / Area (A)	Location (Lon,Lat)
31	Mississippi: Ohio	A	271.70, 40.00 / 282.00, 42.10 279.60, 36.30 / 271.60, 34.00
32	Mississippi: Lower Mississippi/Tennessee	A	271.40, 38.90 / 271.60, 33.30 267.70, 29.60 / 266.00, 37.90
33	Mackenzie: Peel River Basin + Mackenzie Delta	A	223.10, 68.90 / 225.10, 69.50 229.40, 64.00 / 222.10, 64.60
34	Mackenzie: Great Bear Lake sub-basin	A	226.70, 67.50 / 246.70, 66.10 238.90, 61.20 / 230.00, 63.10
35	Mackenzie: Great Slave Lake sub-basin	A	246.70, 66.10 / 254.40, 61.40 240.60, 57.00 / 238.90, 61.20
36	Mackenzie: Liard River basin	A	230.00, 63.10 / 238.90, 61.20 240.60, 57.00 / 229.50, 58.50
37	Mackenzie: Peace River basin east	A	254.40, 61.40 / 254.50, 61.30 240.80, 53.20 / 240.60, 57.00
38	Mackenzie: Peace River basin west	A	232.70, 58.10 / 240.60, 57.00 240.80, 53.20 / 232.70, 56.30
39	Mackenzie: Athabasca River basin	A	254.50, 61.30 / 257.20, 59.10 242.50, 52.10 / 240.80, 53.20
40	Cuenca de la Plata	A	293.50, -24.17 / 301.00, -15.00 318.00, -19.50 / 298.50, -38.50
41	Amazon River: sub-basin 1	A	301.00, 2.50 / 310.00, 1.00 308.50, -15.00 / 301.00, -15.00
42	Amazon River: sub-basin 2	A	288.88, -13.40 / 301.00, -2.67 301.00, -15.00 / 296.50, -20.50
43	Amazon River: sub-basin 3	A	283.50, 4.00 / 299.50, -4.00 286.50, -15.50 / 280.00, -6.00
44	Amazon River: sub-basin 4	A	286.60, 2.50 / 301.00, 5.00 301.00, -2.67 / 299.50, -4.00
45	Amazon River: sub-basin 5	A	286.70, -8.00 / 295.00, -1.80 299.50, -4.00 / 288.98, -13.32
46	Torne River basin	A	17.50, 68.10 / 23.80, 69.80 25.10, 66.40 / 23.10, 65.60
47	Rhone River basin	A	4.60, 48.10 / 7.20, 47.80 7.30, 43.80 / 3.60, 44.00
48	Columbia River basin	A	241.90, 53.30 / 250.70, 43.20 243.30, 41.10 / 238.00, 44.30
49	Colorado River basin	A	241.00, 37.60 / 253.60, 40.90 251.60, 32.30 / 244.60, 31.60
50	Congo River basin	A	12.50, -6.50 / 19.10, 10.70 36.00, -2.90 / 30.50, -13.90
51	Danube River basin	A	8.10, 48.20 / 12.50, 50.40 31.00, 47.00 / 22.00, 41.20
52	Lena River basin	A	104.00, 64.60 / 127.50, 72.00 140.00, 57.30, 111.50, 51.80

**Table 18: Points and areas for the DDH diagnostics**

	Description	Point (P) / Area (A)	Location (Lon,Lat)
53	Mekong River basin	A	96.00, 33.10 / 96.70, 33.50 109.00, 12.80 / 104.60, 10.40
54	Ob River basin	A	59.70, 50.00 / 59.70, 69.50 87.10, 60.00 / 91.50, 48.90
55	Severnaya River basin	A	40.00, 58.60 / 40.60, 65.50 58.80, 61.80 / 59.10, 58.00
56	Yellow River basin	A	96.40, 34.60 / 102.10, 44.90 118.40, 36.90 / 118.60, 31.90
57	Yenisei River basin	A	82.50, 71.80 / 103.50, 65.60 113.30, 48.50 / 91.90, 47.80
58	BALTEX (Baltic Sea run-off area)	A	7.50, 54.00 / 18.00, 70.00 39.00, 62.50 / 22.50, 49.00

6 ECMWF/ISLSCP-II dataset

Plans have been developed with NASA to support Initiative II of the International Satellite Land Surface Climatology Project by providing near surface atmospheric and surface data from ERA40 covering the years 1988 to 1998. ISLSCP-II is an initiative to collect data for use in research on land-surface processes. Relevant ERA-40 data have been interpolated onto the standard 1° ISLSCP grid taking appropriate account of land/sea masks. NASA will produce a CD-ROM and provide other data services for this particular set of products. For information on this dataset see Betts and Beljaars (2003): ECMWF ISLSCP-II near-surface dataset from ERA-40. *ERA-40 Project Report Series*, **8**, 31pp (available from <http://www.ecmwf.int>).

Annex 1. Vertical integrals for energy, mass, water and ozone budgets

The continuous, adiabatic, frictionless form of the model's primitive equations may be manipulated to give the following equations, in standard notation:

Kinetic energy:

$$\begin{aligned} \frac{\partial}{\partial t} \left(E \frac{\partial p}{\partial \eta} \right) = & -\nabla \cdot \left(\underset{\sim}{v} E \frac{\partial p}{\partial \eta} \right) - \nabla \cdot \left(\underset{\sim}{v} \phi - \phi_s \frac{\partial p}{\partial \eta} \right) - \frac{\partial}{\partial \eta} \left(\dot{\eta} E \frac{\partial p}{\partial \eta} \right) + \frac{\partial}{\partial \eta} \left(\phi - \phi_s \int_0^\eta \nabla \cdot \underset{\sim}{v} \frac{\partial p}{\partial \eta} d\eta \right) \\ & - \frac{RT\omega \partial p}{p \partial \eta} - \underset{\sim}{v} \frac{\partial p}{\partial \eta} \cdot \nabla \phi_s \end{aligned} \quad (\text{A1.1})$$

$$E = \frac{1}{2} (\underset{\sim}{v} \cdot \underset{\sim}{v})$$

Potential+Internal energy:

$$\frac{\partial}{\partial t} \left((c_p T + \phi_s) \frac{\partial p}{\partial \eta} \right) = -\nabla \cdot \left(\underset{\sim}{v} (c_p T + \phi_s) \frac{\partial p}{\partial \eta} \right) - \frac{\partial}{\partial \eta} \left(\dot{\eta} (c_p T + \phi_s) \frac{\partial p}{\partial \eta} \right) + \frac{RT\omega \partial p}{p \partial \eta} + \underset{\sim}{v} \frac{\partial p}{\partial \eta} \cdot \nabla \phi_s \quad (\text{A1.2})$$

Mass:

$$\frac{\partial}{\partial t} \left(\frac{\partial p}{\partial \eta} \right) = -\nabla \cdot \left(\underset{\sim}{v} \frac{\partial p}{\partial \eta} \right) - \frac{\partial}{\partial \eta} \left(\dot{\eta} \frac{\partial p}{\partial \eta} \right) \quad (\text{A1.3})$$

Water vapour:

$$\frac{\partial}{\partial t} \left(q \frac{\partial p}{\partial \eta} \right) = -\nabla \cdot \left(\underset{\sim}{v} q \frac{\partial p}{\partial \eta} \right) - \frac{\partial}{\partial \eta} \left(\dot{\eta} q \frac{\partial p}{\partial \eta} \right) \quad (\text{A1.4})$$

Ozone:

$$\frac{\partial}{\partial t} \left(O_3 \frac{\partial p}{\partial \eta} \right) = -\nabla \cdot \left(\underset{\sim}{v} O_3 \frac{\partial p}{\partial \eta} \right) - \frac{\partial}{\partial \eta} \left(\dot{\eta} O_3 \frac{\partial p}{\partial \eta} \right) \quad (\text{A1.5})$$

The notation is as in Simmons and Burridge(1981, *Mon. Wea. Rev.*, **109**, 758-766). The gas constant, R , and specific heat at constant pressure, c_p , vary with specific humidity, q :

$$R = R_d \left(1 + \left(\frac{R_v}{R_d} - 1 \right) q \right) \quad (\text{A1.6})$$

$$c_p = c_{pd} \left(1 + \left(\frac{c_{pv}}{c_{pd}} - 1 \right) q \right) \quad (\text{A1.7})$$

where subscripts d and v denote values for dry air and water vapour respectively.

It should be noted that $(c_p T + \phi_s) \frac{\partial p}{\partial \eta}$ should strictly be interpreted in terms of potential+internal energy only when vertically integrated:

$$\int_0^1 (c_v T + \phi) \frac{\partial p}{\partial \eta} d\eta = \int_0^1 (c_p T + \phi - RT) \frac{\partial p}{\partial \eta} d\eta = \int_0^1 \left(c_p T \frac{\partial p}{\partial \eta} + \frac{\partial}{\partial \eta} (p\phi) \right) d\eta = \int_0^1 (c_p T + \phi_s) \frac{\partial p}{\partial \eta} d\eta \quad (\text{A1.8})$$

Integrating the energy, mass, water vapour and ozone equations in the vertical, they may be written symbolically as:

$$\frac{\partial}{\partial t} KE = -(\nabla \cdot \tilde{F}_{KE}) - (\nabla \cdot \tilde{F}_{\phi - \phi_s}) + C_1 + C_2 \quad (\text{A1.9})$$

$$\frac{\partial}{\partial t} PIE = -(\nabla \cdot \tilde{F}_{PIE}) - C_1 - C_2 \quad (\text{A1.10})$$

$$\frac{\partial}{\partial t} Mass = -(\nabla \cdot \tilde{F}_M) \quad (\text{A1.11})$$

$$\frac{\partial}{\partial t} TCWV = -(\nabla \cdot \tilde{F}_q) \quad (\text{A1.12})$$

$$\frac{\partial}{\partial t} TCO = -(\nabla \cdot \tilde{F}_{O_3}) \quad (\text{A1.13})$$

The vertically integrated variables are:

$$KE = \frac{1}{g} \int_0^1 \frac{1}{2} (\tilde{v} \cdot \tilde{v}) \frac{\partial p}{\partial \eta} d\eta \quad (\text{A1.14})$$

$$PIE = \frac{1}{g} \int_0^1 (c_p T + \phi_s) \frac{\partial p}{\partial \eta} d\eta = CPT + \phi_s Mass \quad (\text{A1.15})$$

$$CPT = \frac{1}{g} \int_0^1 c_p T \frac{\partial p}{\partial \eta} d\eta \quad (\text{A1.16})$$

$$Mass = \frac{1}{g} \int_0^1 \frac{\partial p}{\partial \eta} d\eta = \frac{P_s}{g} \quad (\text{A1.17})$$

$$TCWV = \frac{1}{g} \int_0^1 q \frac{\partial p}{\partial \eta} d\eta \quad (\text{A1.18})$$

$$TCO = \frac{1}{g} \int_0^1 O_3 \frac{\partial p}{\partial \eta} d\eta \quad (\text{A1.19})$$

The fluxes are:

$$\tilde{F}_{KE} = \frac{1}{g} \int_0^1 \tilde{v} \frac{1}{2} (\tilde{v} \cdot \tilde{v}) \frac{\partial p}{\partial \eta} d\eta \quad (\text{A1.20})$$

$$\tilde{F}_{\phi - \phi_s} = \frac{1}{g} \int_0^1 \tilde{v} (\phi - \phi_s) \frac{\partial p}{\partial \eta} d\eta = \tilde{F}_{\phi} - \tilde{F}_{\phi_s} \quad (\text{A1.21})$$

$$\tilde{F}_{\phi} = \frac{1}{g} \int_0^1 \tilde{v} \phi \frac{\partial p}{\partial \eta} d\eta \quad (\text{A1.22})$$

$$\tilde{F}_{\phi_s} = \frac{1}{g} \int_0^1 \tilde{v} \phi_s \frac{\partial p}{\partial \eta} d\eta = \phi_s \tilde{F}_M \quad (\text{A1.23})$$

$$\tilde{F}_{PIE} = \frac{1}{g} \int_0^1 \tilde{v} (c_p T + \phi_s) \frac{\partial p}{\partial \eta} d\eta = \tilde{F}_{CPT} + \phi_s \tilde{F}_M \quad (\text{A1.24})$$

$$\tilde{F}_{CPT} = \frac{1}{g} \int_0^1 \tilde{v} c_p T \frac{\partial p}{\partial \eta} d\eta \quad (\text{A1.25})$$

$$\tilde{F}_M = \frac{1}{g} \int_0^1 \tilde{v} \frac{\partial p}{\partial \eta} d\eta \quad (\text{A1.26})$$

$$\tilde{F}_q = \frac{1}{g} \int_0^1 \tilde{v} q \frac{\partial p}{\partial \eta} d\eta \quad (\text{A1.27})$$

$$\tilde{F}_{O_3} = \frac{1}{g} \int_0^1 \tilde{v} O_3 \frac{\partial p}{\partial \eta} d\eta \quad (\text{A1.28})$$

and the energy conversions are:

$$C_1 = -\frac{1}{g} \int_0^1 \frac{RT\omega \partial p}{p \partial \eta} d\eta \quad (\text{A1.29})$$

$$C_2 = -\frac{1}{g} \int_0^1 \left(\tilde{v} \frac{\partial p}{\partial \eta} \cdot \nabla \phi_s \right) d\eta = -\tilde{F}_M \cdot \nabla \phi_s \quad (\text{A1.30})$$

The two energy equations can also be written:

$$\frac{\partial}{\partial t} KE = -(\nabla \cdot \tilde{F}_{KE}) - (\nabla \cdot \tilde{F}_\phi) + C_1 + C_3 \quad (\text{A1.31})$$

$$\frac{\partial}{\partial t} PIE = -(\nabla \cdot \tilde{F}_{CPT}) - C_1 - C_3 \quad (\text{A1.32})$$

where

$$C_3 = -\nabla \cdot \tilde{F}_{\phi_s} \quad (\text{A1.33})$$

The standard post-processing already produces (see Table 9) the net mass of water vapour (total column water vapour, *TCWV* above) and ozone (total column ozone, *TCO* above) in kg/m² for each grid point. Also available is surface geopotential, ϕ_s , enabling the component $\phi_s Mass$ of *PIE* to be simply computed if *Mass* is known. Note that ϕ_s is a fixed field, so the calculation of $\phi_s Mass$ can be done on monthly means if required.

A constant value, $L=2.5008E+06$ J/kg*K has been used for the latent heat coefficient in the moist static and total energy integrals.

In the enthalpy and energy integrals $C_p = C_{pd}*(1.-q) + C_{vd}*q$ as defined in the IFS documentation

In addition to these fields, analysis and selected forecast values of the following will be archived:

- *KE*, *CPT* and *Mass*
- \tilde{F}_{KE} , \tilde{F}_ϕ , \tilde{F}_{CPT} , \tilde{F}_M , \tilde{F}_q and \tilde{F}_{O_3}
- C_1



These are most directly appropriate for use of the energy equation in the form given by equations (A1.31) and (A1.32). The flux $F_{\sim\phi_s}$ can be simply calculated as $\phi_s F_{\sim M}$, and the conversion term C_3 is given by the convergence of this flux. The vertical integral, $\frac{1}{g} \int_0^1 e \frac{\partial p}{\partial \eta} d\eta$, of a quantity e that is defined by its analyzed or forecast values e_k at the 60 full model levels is evaluated as $\frac{1}{g} \sum_{k=1} e_k \left(p_{k+\frac{1}{2}} - p_{k-\frac{1}{2}} \right)$.

If the alternative form of the energy equations given by (A1.9) and (A1.10) is preferred, the fluxes $F_{\sim\phi-\phi_s}$ and $F_{\sim PIE}$ can be computed simply by subtracting $\phi_s F_{\sim M}$ from $F_{\sim\phi}$ and adding it to $F_{\sim CPT}$. The conversion term C_2 is given by:

$$C_2 = -F_{\sim M} \cdot \nabla \phi_s = -\nabla \cdot F_{\sim\phi_s} + \phi_s \nabla \cdot F_{\sim M} = C_3 + \phi_s \nabla \cdot F_{\sim M} \quad (\text{A1.34})$$

All RHS terms in the budget equations (A1.9) to (A1.13) (or (A1.31), (A1.32), (A1.11), (A1.12) and (A1.13)) can thus be computed in terms of the supplied integrals, applying a divergence operator and simple multiplications where needed. These operations can be carried out either on the instantaneous values or on their monthly means.